



Molecular evolution and structural analyses of proteins involved in metabolic pathways of volatile organic compounds in *Petunia hybrida* (Solanaceae)

Lucas C. Beltrame¹, Claudia E. Thompson² and Loreta B. Freitas¹ 

¹Universidade Federal do Rio Grande do Sul, Departamento de Genética, Laboratório de Evolução Molecular, Porto Alegre, RS, Brazil.

²Universidade Federal de Ciências da Saúde de Porto Alegre, Departamento de Farmacociências, Porto Alegre, RS, Brazil.

Abstract

The association between plants and their pollinators is essential for increasing the diversity in angiosperms. Morphological and physiological traits, mainly floral scent, can influence the pollination dynamics and select pollinators for each plant species. In this work, we studied two proteins involved in producing volatile organic compounds in plants, *coniferyl alcohol acyltransferase* (CFAT) and *benzoyl-CoA:benzyl alcohol/phenyl ethanol benzoyl transferase* (BPBT) genes. We aimed to understand these proteins with respect to evolutionary and structural aspects and functions in Solanaceae using phylogenetic methods and comparative molecular modeling. We used Bayesian inference to describe the proteins' evolutionary history using *Petunia x hybrida* as a query to search for homologs in the Solanaceae family. Theoretical 3D models were obtained for both proteins using *Panicum virgatum* as a template. The phylogenetic tree included several different enzymes with diverse biological roles in Solanaceae, displaying the transferase domain. We identified only one sequence of CFAT in the databases, which belongs to *Petunia x hybrida*, and found several BPBT sequences from the genera *Nicotiana*, *Solanum*, and *Capsicum*. The 3D structures of CFAT and BPBT have two different domains, and we have identified the amino acid residues essential for the enzymatic activity and interaction with substrates.

Keywords: Volatile organic compounds, CFAT, BPBT, Solanaceae, molecular evolution, protein structure.

Received: March 23, 2022; Accepted: October 31, 2022.

Introduction

The interaction between plants and their pollinators is responsible for a large portion of morphological and structural diversity in angiosperms (Lunau, 2004), which, in some cases, drove their speciation (Fregonezi *et al.* 2013). Formerly defined as a set of convergent floral traits (Faegri and van der Pijl, 1979), the floral syndromes are associated with specific pollinator groups (Fenster *et al.*, 2004; Etcheverry and Alemán, 2005) and allow to predict which group will be attracted to a given plant species (Schiestl and Johnson, 2013). Many floral traits, such as shape, size, petal color, nectar production, and fragrance, can play a critical role in the attraction and frequency of pollinators and influence the quality of pollinator's visits. In addition, several volatile compounds produced mainly in petals are involved in the attraction of pollinators (Raguso, 2001; Knudsen and Gershenzon, 2006; Knudsen *et al.*, 2006). These aromatic stimuli are learned more quickly than visual clues (Arenas and Farina, 2014) and may differentially attract certain pollinator species (Huber *et al.*, 2005; Klahre *et al.*, 2011), especially insects.

The floral scent is essential compared to visual cues in pollination systems involving plants and nocturnal insects (Rachensberger *et al.*, 2019). The floral scent profile is also associated, in general, with pollinator species in particular. For

example, plants that emit high levels of benzenoid compounds are related to moths (e.g., Dobson, 2006). Moreover, some species are known for producing deterrent compounds such as isoeugenol and benzyl benzoate to avoid florivory by insects and other animals (e.g., Dudareva *et al.*, 2013). Even some bees are attracted by pollen scent that contains certain specific compounds (e.g., Rodrigues *et al.*, 2018).

The Solanaceae family encompasses species with tremendous economic and ecological significance, including several cultivated species used in food and ornamentation (Olmstead *et al.*, 2008). Different pollination syndromes are observed among Solanaceae species, and morphological traits are relevant to understanding the evolutionary history of these species and predicting pollinator-plant relationships (Knapp, 2010). The floral volatile organic compounds (VOCs) are strong cues for pollinators and herbivores in Solanaceae (Kessler, 2012).

The *Petunia* genus is a charismatic group of wild species distributed in southern South America and the ornamental and widely known *Petunia hybrida* (Stehmann *et al.*, 2009). The *P. hybrida* is one of the most profitable cultivated species globally and a model for plant genetics and physiological studies (Vandenbussche *et al.*, 2016). This commercial plant is an artificial hybrid developed in the 19th century from crossings between *P. axillaris*, a white-flowered and moth-pollinated plant, and the pink and bee-pollinated *P. interior* species (Segatto *et al.*, 2014).

This study focused on two proteins involved in metabolic pathways of production and emission of VOCs, the benzoyl-CoA:benzyl alcohol/phenyl ethanol benzoyl transferase (BPBT; EC 2.3.2.196) and the coniferyl alcohol acyltransferase (CFAT; EC 2.3.1.84). BPBT is involved in VOCs production, such as phenyl-ethyl benzoate and benzyl benzoate; meanwhile, CFAT converts coniferyl alcohol into coniferyl acetate, a precursor of eugenol and isoeugenol VOCs (Dudareva *et al.*, 2013; Amrad *et al.*, 2016). BPBT and CFAT proteins are members of the large enzymatic family named BAHD (an acronymous of the first four characterized proteins in this group). BAHD are acyltransferases and utilize CoA thioesters to catalyze the formation of several plant secondary metabolites (D'Auria, 2006), including VOCs. BPBT and CFAT are represented by one copy in *P. hybrida* (Dexter *et al.*, 2007).

Previous studies showed that the proteins from the BAHD family fall broadly into five main clades (Tuominen *et al.*, 2011) and contain two conserved protein motifs, HxxxD and DFGWG, which have facilitated *in silico* identification of BAHD acyltransferases from available genome sequences (Luo *et al.*, 2007; Yu *et al.*, 2009; Tuominen *et al.*, 2011). The HxxxD motif is involved in the catalytic activity, whereas DFGWG has a structural role that promotes the stable folding of the protein (Ma *et al.*, 2005). However, even sharing the active motifs and included in the same enzymatic family, BPBT and CFAT proteins can perform many different reactions, acting with a broad spectrum of substrates with low specificity (Wang *et al.*, 2021).

Our main aim was to better understand the evolutionary history of BPBT and CFAT proteins in the Solanaceae family using phylogenetic methods and comparative molecular 3-D modeling with an emphasis on *P. hybrida* sequences. In addition, we based our study on the hypothesis that these proteins have evolved by convergence regarding the VOC type that each one produces and the preferential group of pollinators attracted by the plant species.

Material and Methods

Sequences retrieval and alignment

We used BLAST searches with default parameters to obtain homologous protein sequences (PhBPBT and PhCFAT) from the public sequence database National Center for Biotechnology Information (NCBI Resource Coordinators, 2016; NCBI, 2022) using *Petunia hybrida* BPBT and CFAT protein sequences as queries (GenBank ID: AAU06226.1 and ABG75942.1, respectively). We analyzed the protein domains using the *hmmscan* tool in HMMER (Finn *et al.*, 2011; HMMER, 2020) software against Pfam (Finn *et al.*, 2016; Pfam, 2022) database with default parameters. The next step was to identify the HMM (Hidden Markov model) profile and generate a local database including all sequences with a similar profile using the *hmmsearch* tool from HMMER against the UniProtKB database (The UniProt Consortium, 2017) with default parameters. We restricted the results to include only sequences from Solanaceae species; as a result, we retrieved all protein sequences with the same HMM profile.

We used BLAST+ (Camacho *et al.*, 2009) software to format a local database using the sequences previously

identified and searched for homologs using a specific cutoff (e-value $\leq 10^{-6}$). We downloaded the sequences in FASTA format from the list of sequences that matched these criteria and excluded all partial sequences. Subsequently, we performed the alignment using the PRANK (Löytynoja and Goldman, 2005; PRANK, 2022) software with default parameters. The alignment was manually edited using AliView software (Larsson, 2014; AliView, 2021), excluding ambiguous positions.

Molecular genealogy

We used ProtTest (Abascal *et al.* 2005) with default settings to choose the best-fit models of amino-acid replacement based on AIC (Akaike's information criterion), BIC (Bayesian information criterion), AICc (AIC with a correction for finite sample sizes), and DTC (Decision Theory criterion) criteria. We obtained a phylogenetic tree for acyltransferases (including the BPBT and CFAT proteins) using the probabilistic Bayesian inference method in MrBayes software (Ronquist *et al.*, 2011; MrBayes, 2019) with default parameters and the best evolutionary model. We ran four chains for 2,000,000 generations and discarded 25% of the genealogies as burn-in.

Structural analyses

To theoretically model the previously published BPBT and CFAT proteins from *P. hybrida* (PhCFAT GenBank ID: ABG75942.1; PhBPBT, GenBank ID: AAU06226.1), we downloaded the FASTA sequences and used them as queries for searching homologs with identified three-dimensional structures using the BLAST tool (Altschul *et al.*, 1990) against the Protein Data Bank (Berman *et al.*, 2000; PDB, 2022).

We used the resolution equal to or higher than 2.0 Å, identity higher than 25 %, and high coverage as the criteria to choose the best template for the comparative molecular modeling (Sánchez and Sali, 1997; Wiltgen, 2018). In addition, we ran the MAFFT software (Katoh and Standley, 2013; MAFFT, 2021) with default parameters to align queries and templates and inspect the coverage among them. After identifying the best templates, we used MODELLER software (Sali and Blundell, 1993; Webb and Sali, 2014; MODELLER, 2022) to model the three-dimensional structures of PhBPBT and PhCFAT proteins.

We used the PROCHECK (Laskowski *et al.*, 1993; PROCHECK, 2010) and Verified 3D (Lüthy *et al.*, 1992) software to verify each generated model's quality and stereochemical parameters. An essential criterion for choosing the best model is the number of residues within the most favored and additional allowed regions identified on the Ramachandran plots (Ramakrishnan and Ramachandran, 1965; Morris *et al.*, 1992) generated by PROCHECK. These regions are based on plotting the dihedral angles ψ (psi) and Φ (phi) of each residue of the protein main chain evaluating which bonds between residues are spatially and structurally favored. The lowest number of residues with geometric distortions is also helpful in choosing the best model. We obtained the theoretical isoelectric point using the ExPASy Tools software (Gasteiger *et al.*, 2005; ExPASy, 2020). Finally, we generated figure models using the PyMol software (2022), including each protein's electrostatic potential.

Results

Sequence retrieval and alignment

The search for BPBT and CFAT proteins recovered enzymes with a transferase domain starting at the 11th site and ending at the 441st site for BPBT and from the 6th to 438th sites for CFAT. We found 807 sequences per query from Solanaceae taxa, resulting in 502 and 501 homologous sequences for PhBPBT and PhCFAT proteins, respectively, after filtering by HSP (high scoring pairs) with a permissive e-value = 10 (Table S1). The same proteins were simultaneously recovered with both queries when all sequences were compared. All repeated IDs were then discarded. We applied a threshold of at least 25% identity to select the final data set and excluded

partial sequences, resulting in 335 sequences identified in the UniProtKB AC/ID database. These sequences were aligned, and all ambiguous positions were manually excluded. The final alignment included 1,578 amino acid residues.

Phylogenetic tree construction

The best-fit evolutionary model for this data set was J.T.T. + I + G [Jones-Taylor-Thornton (Jones *et al.*, 1992) + Invariant sites + Gamma distribution]. A phylogenetic tree was obtained, representing all Solanaceae acyltransferase proteins with high posterior probability values for the branches (mainly PP > 0.80), especially ancient events. The tree had two main clades grouping different proteins with the transferase domain (Figure 1).

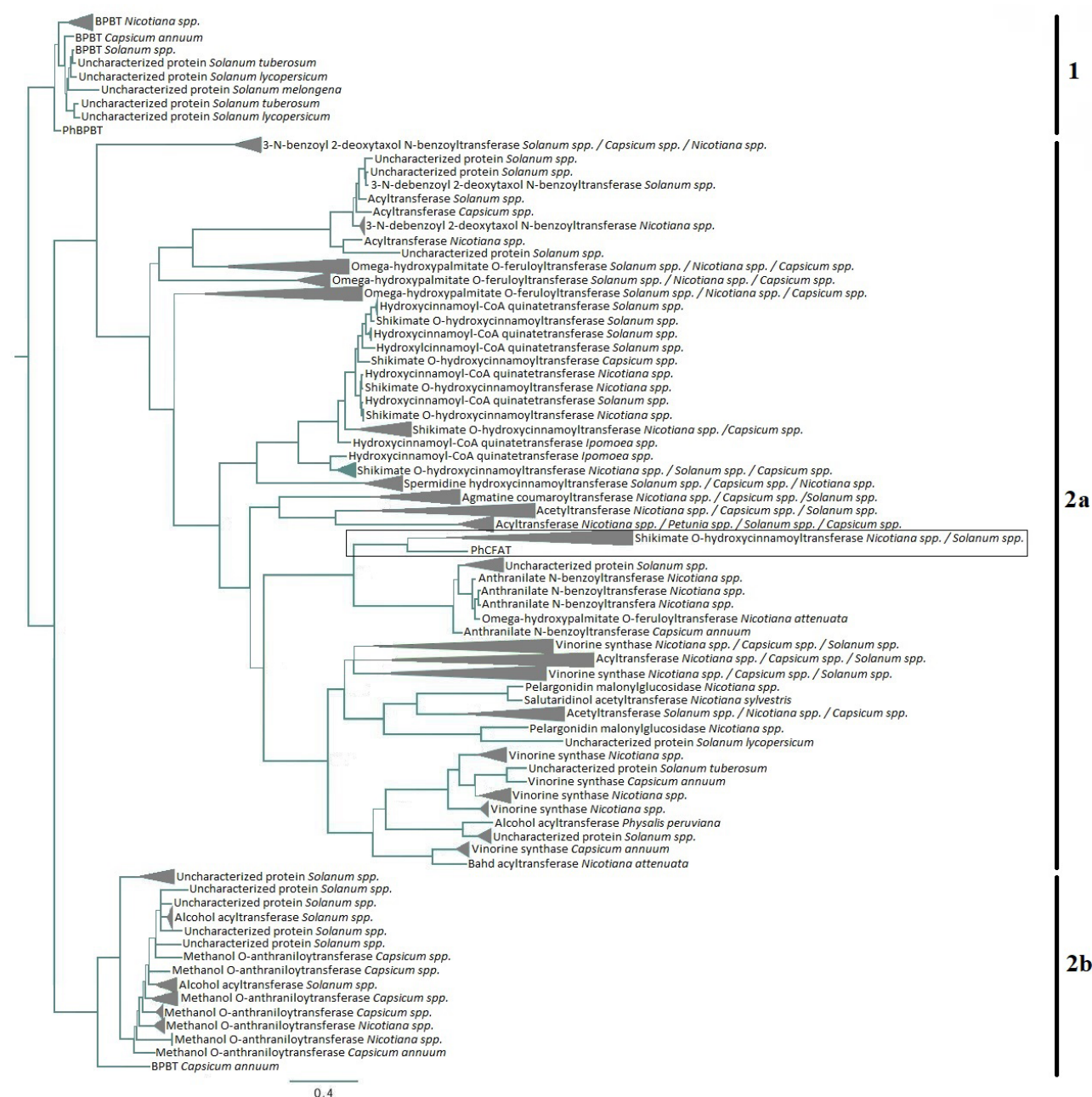


Figure 1 - Solanaceae protein with transferase domain simplified phylogenetic tree generated using Bayesian Inference and JTT + I + G as evolutionary method and model, respectively. The analysis included BPBT and CFAT sequences. Branches with more than one sequence from the same genus were collapsed and indicated with *spp.* Wider branches indicate PP > 0.80 while narrowed branches had PP < 0.80. The rectangle highlights PhCFAT relationships.

Clade 1 included BPBT sequences from *Nicotiana*, *Capsicum*, *Solanum*, the *Petunia hybrida* BPBT (PhBPBT), and other proteins with no characterized function from *Solanum* species. PhBPBT was the sister group of the remaining sequences, and all BPBT sequences from *Nicotiana* species were grouped (PP = 1.0). Only one BPBT sequence was not included in this clade (an isoform observed in *Capsicum annuum*, see below). The uncharacterized sequences of *Solanum* species grouped with *Solanum* BPBT (PP = 0.93) suggesting that even displaying some differences among species, these proteins are at least BPBT-like. The *C. annuum* BPBT sequence was the sister group of *Solanum* sequences. Different insect groups pollinate these species, and the relationships among BPBT sequences were compatible with the genera phylogenetic position.

Clade 2 included PhCFAT, a *C. annuum* BPBT isoform, multiple transferase proteins involved in different metabolic pathways, such as phenylpropanoids' biosynthesis (mainly hydroxycinnamic acid amides - HCAAs), and several uncharacterized proteins from wild and cultivated species in *Solanum*, *Capsicum*, *Nicotiana*, *Ipomoea*, *Lycianthes*, *Datura*, and *Physalis* genera. This clade was subdivided into two main subclades. The subclade 2a grouped proteins with varied functions disposed on minor clades mainly based on their specific activity. Some of these proteins indicated ancient duplications, mainly in *Nicotiana*, *Solanum*, and *Capsicum*, the most studied genera. Subclade 2b encompassed BPBT isoform of *C. annuum* as the sister group of *Solanum* uncharacterized proteins and *Solanum*, *Capsicum*, and *Nicotiana* methanol and alcohol transferases.

Protein 3D structure

Using the previously published PhBPBT and PhCFAT protein sequences as queries to search for homologs with three-dimensional (3D) structures previously determined, we obtained nine hits for BPBT and eight for CFAT. Based on the criteria of highest coverage, identity, and resolution, we selected the crystal structure of *Panicum virgatum* shikimate hydroxycinnamoyl transferase (HCT) in complex with Coa and P-coumaroyl-shikimate (PvHCT2a; PDB ID: 5FAL,

chain A; Eudes *et al.* 2016b) as a template for modeling BPBT and CFAT proteins in *P. hybrida*. The selected template had a resolution of 1.9 Å, with 30% of identity and 96% of coverage to BPBT, 29% of identity and 95% of coverage to CFAT. As we observed that PhCFAT is evolutionarily close to a monophyletic group of HCT from different species (Figure 1), it is justified to use a shikimate hydroxycinnamoyl transferase to model both CFAT and BPBT proteins.

The comparative molecular modeling generated 10 models for PhBPBT and PhCFAT proteins (see Table 1 for the main stereochemical data for all models). First, we evaluated the Ramachandran plot obtained in the PROCHECK to obtain information about the residues within the most favored, additional allowed, generously allowed, and disallowed regions (Table 1). All models showed more than 95% of the amino acid residues in the most favored and additional allowed regions. According to the stereochemical analyses, we chose model 8 (Figure 2A) and model 3 (Figure 2B) as the best models for PhBPBT and PhCFAT proteins, respectively, as both showed high and positive scores for the sum of the 3D profile based on the Verify 3D (2021) analysis. Additionally, the G-factor values were -0.20 for PhBPBT and -0.29 for PhCFAT, indicating minor and insignificant geometric troubles in the model configuration.

We inspected the final models 8 and 3 to identify the protein domains and the amino acid residues that are functionally important by aligning the models and template. The active site and the substrate-binding regions of the template were identified on the models (Table 2). We identified two domains in the template: the first domain contained amino acid residues 1-199 and 387-409, whereas the second comprised the regions between 200-386 and 410-446. Two distinct domains were also identified in the modeled PhBPBT structure (Figure 3A); domain I comprised the residues 1-204 and 376-401, whereas domain II encompassed the residues 205-375 and 402-460. Similarly, the modeled PhCFAT (Figure 3B) also showed two different domains, the first was equivalent to the residues 1-193 and 378-402, and the second domain was formed by amino acid residues 194-377 and 403-454.

Table 1 – Stereochemical data for all 3-D generated models for PhBPBT and PhCFAT proteins.

Model	BPBT									CFAT									
	Ramachandran				Distortions				G-factors	Model	Ramachandran				Distortions				G-factors
	F+AF	F	AF	GA	D	TL	Plan	DA	Overall		F+AF	F	AF	GA	D	TL	Plan	DA	Overall
1	97.9	89.4	8.5	1.5	0.5	21	1	17	-0.20	1	97.3	86.5	10.8	1.8	1.0	44	0	30	-0.33
2	98	87.9	10.1	0.8	1.3	16	0	12	-0.17	2	97.3	86.5	10.8	1.5	1.2	25	0	24	-0.29
3	96.9	86.6	10.3	2.6	0.5	18	0	11	-0.20	3	97.2	86.0	11.2	1.5	1.2	29	0	21	-0.29
4	98.4	88.9	9.5	1.0	0.5	18	0	12	-0.20	4	96.5	86.0	10.5	2.5	1.0	35	0	20	-0.30
5	97.9	87.6	10.3	1.0	1.0	24	0	22	-0.21	5	96.7	86.5	10.2	1.8	1.5	38	0	26	-0.28
6	97.7	88.9	8.8	1.0	1.3	22	1	14	-0.20	6	97.2	86.2	11.0	2.0	0.8	33	0	23	-0.31
7	98.4	89.9	8.5	0.8	0.8	20	2	14	-0.18	7	97.0	85.5	11.5	2.2	0.8	35	0	29	-0.32
8	98.2	89.4	8.8	1.3	0.5	25	1	16	-0.20	8	95.3	86.8	9.5	2.2	1.5	39	0	23	-0.31
9	98.2	87.4	10.8	0.5	1.3	20	1	20	-0.21	9	97.2	86.2	11.0	1.2	1.5	30	0	18	-0.27
10	97.9	89.4	8.5	1.5	0.5	21	1	17	-0.20	10	97.5	87.0	10.5	1.0	1.5	34	0	25	-0.32

F = % residues in most favored regions; AF = % residues in additional allowed regions; GA = % residues in generously allowed regions; D = % residues in disallowed regions; TL = number of bond lengths distortions within main-chain; Plan = number of distortions in planar groups; DA = number of bond angle distortions within the main-chain. Bold values indicate the best model.

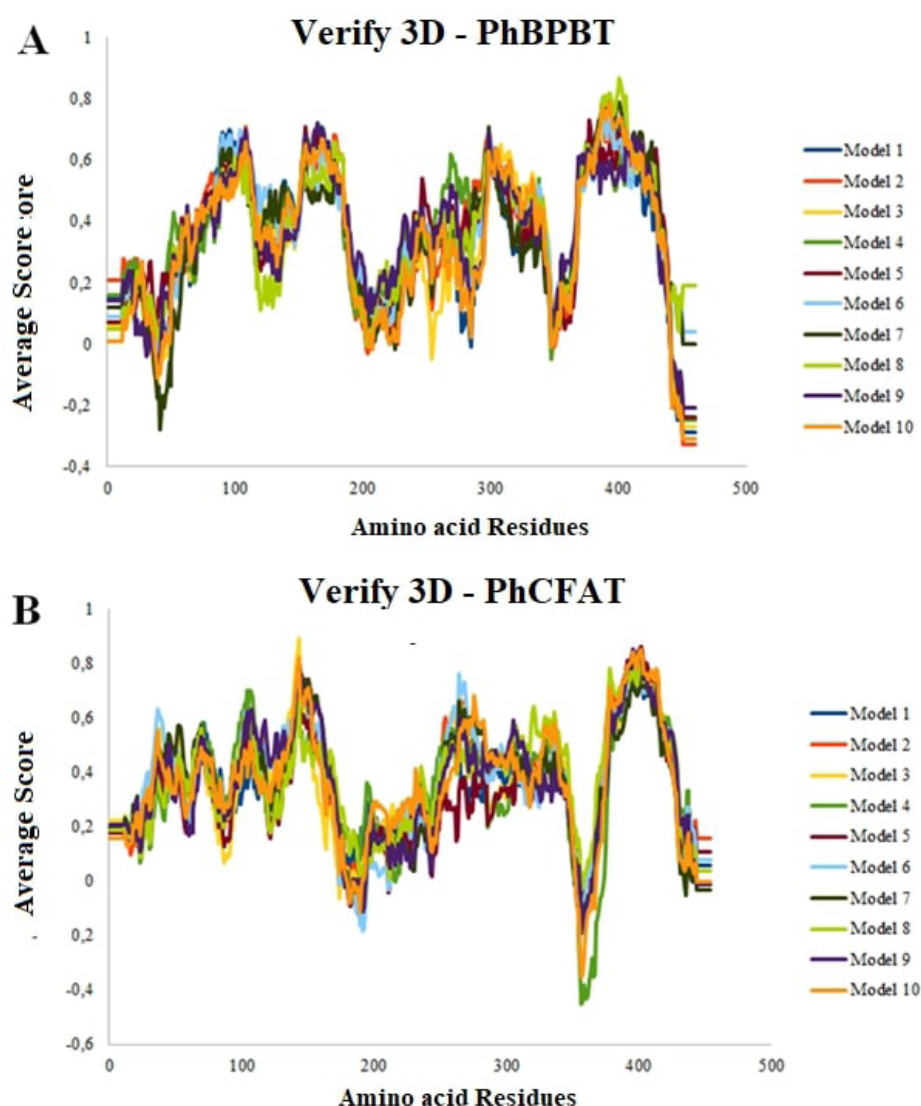


Figure 2 - Evaluation of theoretical 3-D models using Verify 3D for *Petunia hybrida*. (A) PhBPBT protein sequence; (B) PhCFAT protein sequence.

Table 2 – Amino acid residues described as important for the protein function in template (PDB ID: 5FAL A) and their correspondent positions in the modelled PhBPBT and PhCFAT proteins.

Template (5FAL A)			BPBT (Model 8)			CFAT (Model 3)		
AA ¹	P ²	Classification	AA ¹	P ²	Classification	AA ¹	P ²	Classification
Arg	369	Polar + Charged	Lys	357	Polar + Charged	Lys	357	Polar + Charged
Thr	382	Polar Uncharged	Val	370	Non-polar	Ser	373	Polar Uncharged
His	163	Polar + Charged	His	167	Polar + Charged	His	155	Polar + Charged
Trp	384	Non-polar	Asp	372	Polar - Charged	Gly	375	Non-polar
Ser	38	Polar Uncharged	Val	40	Non-polar	Gly	43	Non-polar
Tyr	40	Polar Uncharged	Asn	51	Polar Uncharged	Phe	45	Non-polar

¹Three-letters amino acid abbreviation; ²Amino acid position at the protein sequence; Arg - Arginine; Thr - Threonine; His - Histidine; Trp - Tryptophan; Ser - Serine; Tyr - Tyrosine; Lys - Lysine; Val - Valine; Asp - Aspartic acid; Asn - Asparagine; Gly - Glycine; Phe - Phenylalanine. The 3D structures of PhBPBT and PhCFAT were aligned with the template structure using the PyMol software.

The two domains had a core β -sheet surrounded by α -helices. In the PhBPBT 3D model, we found seven α -helices and nine β -sheets in domain I and nine α -helices and seven β -sheets in the second domain (Figure 3A). The modeled PhCFAT showed seven α -helices and a core containing seven β -sheets in domain I, while the domain II held ten α -helices and six β -sheets (Figure 3B). The structural alignment between the template and modeled PhBPBT (Figure 4A) and PhCFAT (Figure 4B) showed differences in their electrostatic potentials, with the most significant differences in the domain II and active site regions (Figure 5). PhBPBT and PhCFAT had pI (isoelectric point) = 3.79 and pI = 5.57, respectively. In contrast, the template PvhCT2a showed a pI = 5.52.

In the template, the two domains had substrate-binding sites responsible for interacting with molecules that participate in the reaction catalyzed by PvhCT2a from *Panicum virgatum*, suggesting that each domain of PhCFAT and PhBPBT may have similar interactions with their respective substrates. Based on the structural alignment among models and template, we could identify the amino acid residues potentially involved in the enzyme-substrate interactions (Table 2).

We also identified some amino acid substitutions in each protein that could change the physicochemical properties of some amino acids (Table 2). In PhBPBT, the main changes were found in residues 370, 372, and 40, whereas in PhCFAT were in residues 45 and 43.

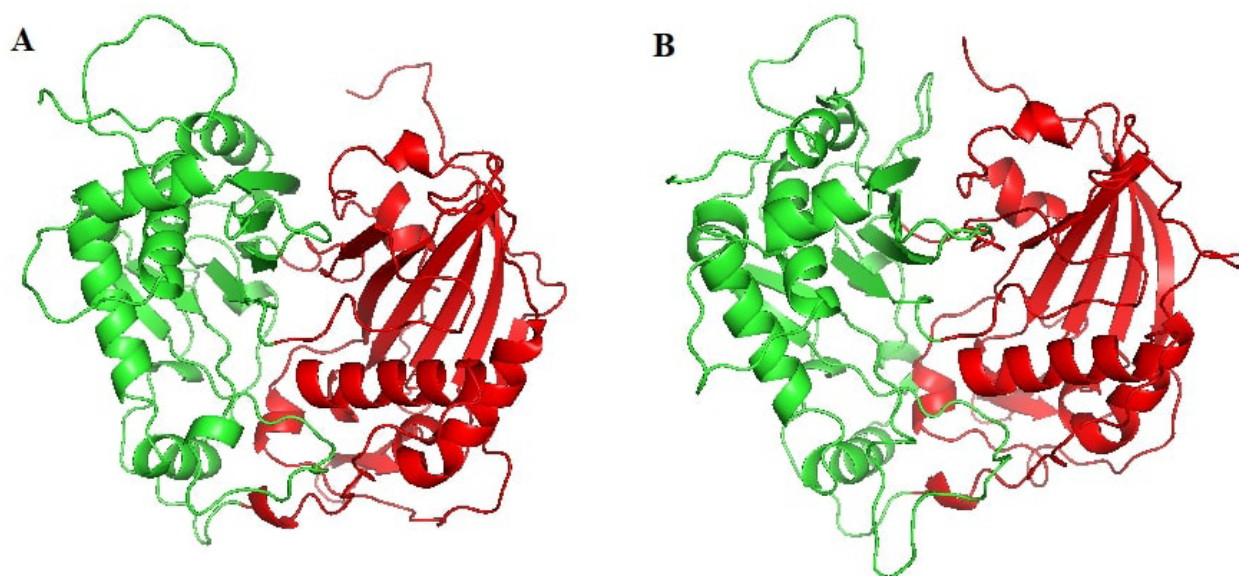


Figure 3 - Cartoon representation for the 3-D structure of modeled proteins of *Petunia hybrida* colored per domain (Red = Domain I; Green = Domain II): (A) PhBPBT protein sequence; (B) PhCFAT protein sequence.

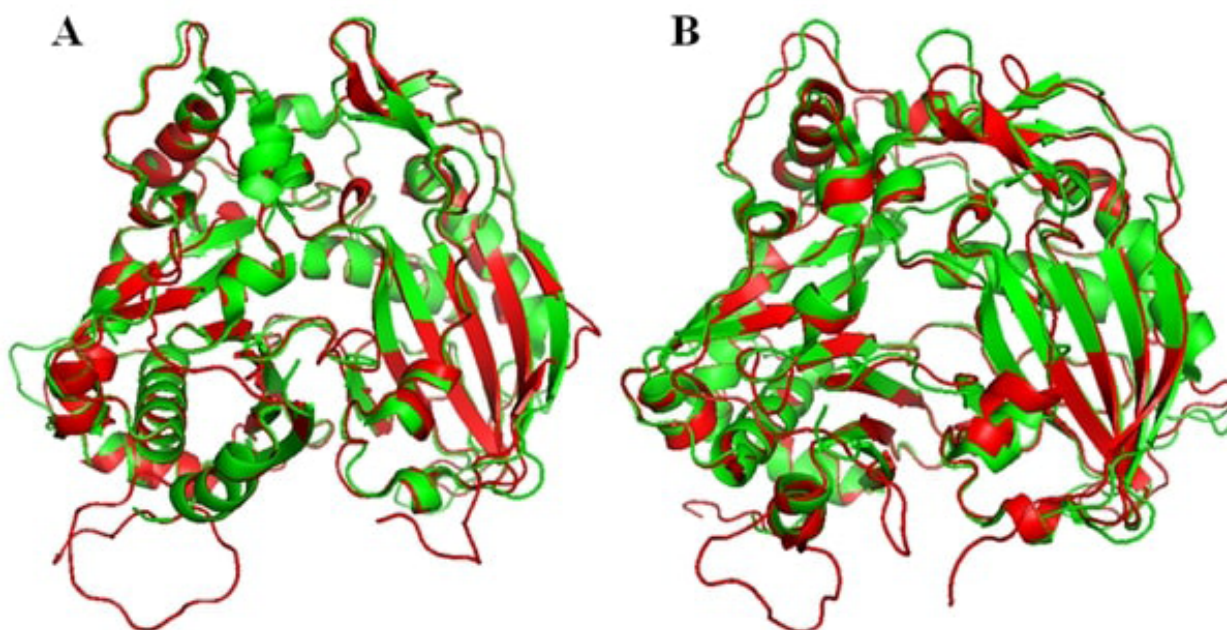


Figure 4 - Cartoon representation for the superimposition between the 3-D *Petunia hybrida* structures and *Panicum virgatum* template: (A) PhBPBT sequence; (B) PhCFAT sequence. The template is represented in green, BPBT and CFAT in red.

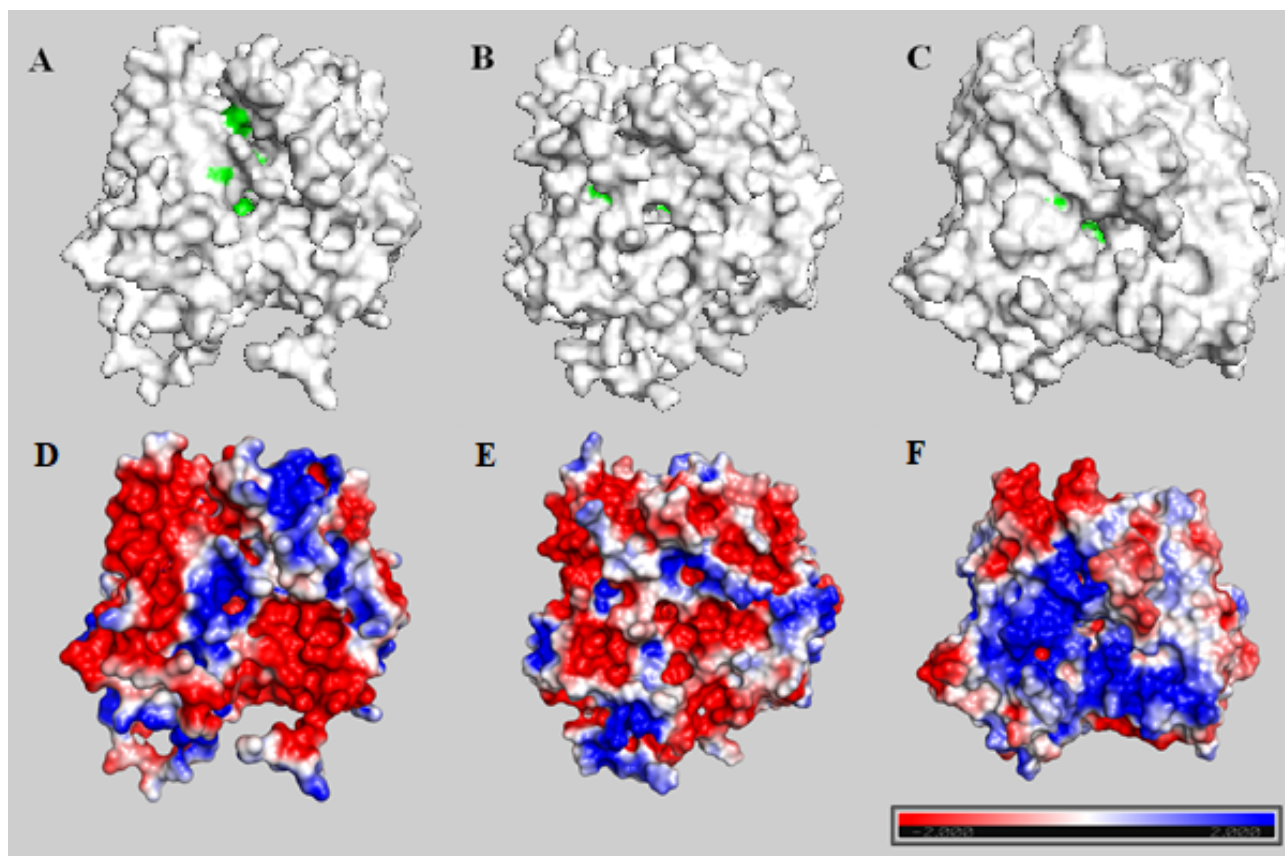


Figure 5 - Molecular surface of PhBPBT (A, D), PhCFAT (B, E), and PvHCT2a (C, F) indicating the active sites (green) and their electrostatic potential, respectively. The most negative residues were colored in red, the neutral in white, and the most positive in blue.

Discussion

We described the evolutionary relationships between homologous sequences of two Solanaceae transferases involved in volatile organic compounds' synthesis. We also modeled the tridimensional structure of these two proteins for *Petunia hybrida*.

Our results indicated that BPBT and CFAT proteins are proximately related, and both sequences of *P. hybrida*, when used as queries, recovered the same homologous protein sets. Most BPBT sequences integrated the same clade, whereas CFAT sequences grouped with other transferases from different nightshade genera. Our molecular genealogy showed proteins preferentially grouped due to their activities. In addition, several proteins seem to result from gene duplications, as many diploid species displayed multiple copies of these proteins (Figure 1; e.g., shikimate O-hydroxynamoyltransferase of *Capsicum* and *Nicotiana* that appeared in different branches in the tree). The 3D modeling reflected the structural similarity between PhBPBT and PhCFAT and indicated their functional differences.

PhBPBT and PhCFAT proteins are involved in isoeugenol biosynthesis, a phenylpropanoid volatile and prominent component of floral scent in *Petunia* (Koeduka *et al.*, 2006). Among wild petunias, only *P. axillaris* has scented petals (Stehmann *et al.*, 2009) and attracts hawkmoths (Venail *et al.*, 2010). Some *P. hybrida* lineages and cultivars also produce aroma (Fenske *et al.*, 2015), with isoeugenol as the final product

in a pathway that starts with phenylalanine (Phe). In this way, CFAT acetylates coniferyl alcohol to produce coniferyl acetate (Dexter *et al.*, 2007), and BPBT catalyzes a reaction that combines benzyl alcohol and benzoyl-CoA (Boatright *et al.*, 2004) internally (Clark *et al.*, 2009). The shikimic acid pathway precedes the phenylpropanoid biosynthesis (Orlova *et al.*, 2006), and the shikimate O-hydroxycinnamoyl transferase is a crucial enzyme in this process in tobacco (Hoffmann *et al.*, 2004). In Figure 1, we reported that PhCFAT and *Nicotiana* and *Solanum* shikimate O-hydroxycinnamoyl transferase are sister proteins, which could be explained, at least in part, by the relationships of these proteins in the same pathway that could have derived from the same ancestor by duplication and neofunctionalization, similar to other proteins that integrate a same metabolic route (e.g., Maere *et al.*, 2005; Yockteng *et al.*, 2013). However, our search did not recover a sequence for *P. hybrida* shikimate O-hydroxycinnamoyl transferase that was recently identified (Kim *et al.*, 2019). However, until the PhHCT discovery, BPBT and CFAT were the only known BAHD family members in *Petunia* (Dexter *et al.*, 2007).

We also verified some gene duplication in these proteins, even among diploid species. Many of these duplicated proteins play different functions, which suggests duplication followed by neofunctionalization in the BAHD family. Neofunctionalization due to punctual duplications in Solanaceae has been observed among other proteins (e.g., Segatto *et al.*, 2016a,b).

Analyzing the *Prunus mume* BAHD family (Zhang *et al.*, 2019), the authors included PhBPBT and PhCFAT sequences in the comparisons and identified 20 conserved motifs. PhBPBT and PhCFAT showed 13 and 12 motifs, respectively, with shared order but different positions and lengths. Motif 2 contained the HxxxD, and motif 3 had the DFHWG domain, both present in all groups of sequences. In that analysis, PhBPBT and PhCFAT integrated different clades with a similar composition to that we obtained here. Other phylogenetic analyses based on BADH family sequences have also had similar results (Yu *et al.*, 2009; Tuominen *et al.*, 2011).

The phylogenetic position of PhBPBT and PhCFAT and their sister sequences in respective clades agree with the evolutionary relationships between genera in Solanaceae (Särkinen *et al.*, 2013) and the time of genome origins. The *Petunia* genome was the first to diverge, followed by *Nicotiana*, *Capsicum*, and *Solanum* (Bombarely *et al.*, 2016). This concordance suggests that multiple copies observed in other genera and not in *P. hybrida* for BPBT and CFAT were acquired posteriorly to the genera divergence and, due to *Petunia* species, in general, are not scented (Amrad *et al.*, 2016), the copy number of each gene in the BAHD family was limited in *P. hybrida*.

Regarding the 3D models, our results showed that the modeled PhBPBT and PhCFAT proteins have a high identity (29% and 30%, respectively) and the same overall 3D fold (Figure 3) and are very similar to the *Panicum virgatum* shikimate hydroxycinnamoyl transferase. Despite the structural similarities, these three proteins differ in surface properties (Figure 4; Table 2). The three modeled proteins show two domains and some mutations in the active site that indicate differences in their interaction with the substrate and activities.

The Arg369, Thr382, His163, Trp384, Ser38, and Tyr40 residues are implicated in the interactions with substrates in the active site of PvHCT2a (Eudes *et al.* 2016a). These residues corresponded to the amino acid residues Lys357, Val370, His167, Asp372, Val40, and Asn51 in the PhBPBT, whereas for PhCFAT, these PvHCT2a residues were structurally aligned to Lys357, Ser373, His155, Gly375, Gly43, and Phe45 sites. Comparing the physicochemical properties of these residues among template and models, we could evaluate the impact of the amino acid substitutions in each protein. The results indicated that some mutations in the active site region changed the physicochemical properties of some amino acids (Table 2). These structural changes observed in PhBPBT and PhCFAT proteins suggested that functional changes, such as different polarity and charges of specific amino acids, may alter functional aspects of these proteins, mainly regarding the substrate specificity.

Our results support a shared mechanism of pollinator attraction in different steps of the volatile pathway of flowers of nightshades. Identifying and characterizing these key components would provide valuable tools for future discoveries in wild species and understanding their plant-pollinator interactions.

Acknowledgements

This work was supported by the Conselho Nacional de Desenvolvimento Científico e Tecnológico (CNPq),

Coordenação de Aperfeiçoamento de Pessoal de Nível Superior (CAPES), and Programa de Pós-Graduação em Genética e Biologia Molecular da Universidade Federal do Rio Grande do Sul (PPGBM-UFRGS).

Conflict of Interests

The authors declare that they have no conflict of interest.

Author Contributions

CET and LBF planned, designed, and led the project; LCB and CET obtained data and ran the analyses; LBF led the manuscript preparation. All authors have commented on and approved the final manuscript.

References

- Abascal F, Zardoya R and Posada D (2005) ProtTest: selection of best-fit models of protein evolution. *Bioinformatics* 21:2104-2105.
- Altschul SF, Gish W, Miller W, Myers EW and Lipman DJ (1990) Basic local alignment search tool. *J Mol Biol* 215:403-410.
- Amrad A, Moser M, Mandel T, de Vries M, Schuurink RC, Freitas L and Kuhlemeier C (2016) Gain and loss of floral scent production through changes in structural genes during pollinator-mediated speciation. *Curr Biol* 26:3303-3312.
- Arenas A and Farina WM (2014) Bias to pollen odors is affected by early exposure and foraging experience. *J Insect Physiol* 66:28-36.
- Berman HM, Westbrook J, Feng Z, Gilliland G, Bhat TN, Weissig H, Shindyalov IN and Bourne PE (2000) The protein data bank. *Nucl Acids Res* 28:235-242.
- Boatright J, Negre F, Chen X, Kish CM, Wood B, Peel G, Irina I, Gang D and Dudareva N (2004) Understanding in vivo benzenoid metabolism in *Petunia* petal tissue. *Plant Physiol* 135:1993-2011.
- Bombarely A, Moser M, Amrad A, Amrad A, Bao M, Bapaume L, Barry CS, Bliet M, Boersma MR, Borghi L *et al.* (2016) Insight into the evolution of the Solanaceae from the parental genomes of *Petunia hybrida*. *Nat Plants* 2:16074
- Camacho C, Coulouris G, Avagyan V, Ma N, Papadopoulos J, Bealer K and Madden TL (2009) BLAST+: architecture and applications. *BMC Bioinformatics* 10:421.
- Clark DG, Pichersky E, Verdonk J, Dudareva N, Haring M, Klahre U and Schuurink R (2009) Benzenoids dominate the fragrance of *Petunia* flowers. In: Gerats T, Strommer J (eds) *Petunia: evolutionary, developmental and physiological genetics*. Springer, New York, pp 51-69.
- D'Auria JC (2006) Acyltransferases in plants: A good time to be BAHD. *Curr Opin Plant Biol* 9:331-340.
- Dexter R, Qualley A, Kish CM, Ma CJ, Koeduka T, Nagegowda DA, Dudareva N, Pichersky E and Clark D (2007) Characterization of a petunia acetyltransferase involved in the biosynthesis of the floral volatile iso Eugenol. *Plant J* 49:265-275.
- Dobson HEM (2006) Relationship between floral fragrance composition and type of pollinator. In: Dudareva N, Pichersky E (eds) *Biology of floral scent*. Taylor and Francis, Boca Raton, pp 147-198.
- Dudareva N, Klempien A, Muhlemann JK and Kaplan I (2013) Biosynthesis, function and metabolic engineering of plant volatile organic compounds. *New Phytol* 198:16-32.
- Etcheverry AV and Alemán CET (2005) Reproductive biology of *Erythrina falcata* (Fabaceae: Papilionoideae). *Biotropica* 37:54-63.
- Eudes A, Mouille M, Robinson DS, Benites VT, Wang G, Roux L, Tsai YL, Baidoo EEK, Chiu TY, Heazlewood JL *et al.* (2016a) Exploiting members of the BAHD acyltransferase family to

- synthesize multiple hydroxycinnamate and benzoate conjugates in yeast. *Microb Cell Fact* 15:198.
- Eudes A, Pereira JH, Yogiswara S, Wang G, Benites VT, Baidoo EEK, Lee TS, Adams PD, Keasling JD and Loqué D (2016b) Exploiting the substrate promiscuity of hydroxycinnamoyl-CoA:shikimate hydroxycinnamoyl transferase to reduce lignin. *Plant Cell Physiol* 57:568-579.
- Faegri K and van der Pijl L (1979) The principles of pollination ecology. Pergamon Press, Oxford. 242 p.
- Fenske MP, Hewett-Hazelton KD, Hempton AK, Shim JS, Yamamoto BM, Riffell JA and Imaizumi T (2015) Circadian clock gene *LATE ELONGATED HYPOCOTYL* directly regulates the timing of floral scent emission in *Petunia*. *Proc Natl Acad Sci U S A* 31:9775-9780.
- Fenster CB, Armbruster WS, Wilson P, Dudash MR and Thomson JD (2004) Pollination syndromes and floral specialization. *Annu Rev Ecol Evol Syst* 35:375-403.
- Finn RD, Clements J and Eddy SR (2011) HMMER Web Server: interactive sequence similarity searching. *Nucleic Acids Res* 38:W29-W37.
- Finn RD, Coghill P, Eberhardt RY, Eddy SR, Mistry J, Mitchell AL, Potter SC, Punta M, Qureshi M, Sangrador-Vegas A *et al.* (2016) The Pfam protein families database: towards a more sustainable future. *Nucleic Acids Res* 44:D279-D285.
- Fregonezi JN, Turchetto C, Bonatto SL and Freitas LB (2013) Biogeographical history and diversification of *Petunia* and *Calibrachoa* (Solanaceae) in the Neotropical Pampas grassland. *Bot J Lin Soc* 171:140-153.
- Gasteiger E, Hoogland C, Gattiker A, Duvaud S, Wilkins MR, Appel RD and Bairoch A (2005) Protein identification and analysis tools on the ExPASy Server. In: Walker JM (ed). *The proteomics protocols handbook*. Humana Press, Totowa, pp 571-607.
- Hoffmann L, Besseau S, Geoffroy P, Ritzenthaler C, Meyer D, Lapierre C, Pollet B and Legrand M (2004) Silencing of hydroxycinnamoyl-coenzyme A shikimate/quinic hydroxycinnamoyl transferase affects phenylpropanoid biosynthesis. *Plant Cell* 16:1446-1465.
- Huber FK, Kaiser R, Sauter W and Schiestl FP (2005) Floral scent emission and pollinator attraction in two species of *Gymnadenia* (Orchidaceae). *Oecologia* 142:564-575.
- Jones DT, Taylor WR and Thornton JM (1992) The rapid generation of mutation data matrices from protein sequences. *Comput Appl Biosci* 8:275-282.
- Katoh K and Standley DM (2013) MAFFT multiple sequence alignment software version 7: improvements in performance and usability. *Mol Biol Evol* 30:772-780.
- Kessler D (2012) Context dependency of nectar reward-guided oviposition. *Entomol Exp Appl* 144:112-122
- Klahre U, Gurba A, Hermann K, Saxenhofer M, Bossolini E, Guerin PM and Kuhlemeier C (2011) Pollinator choice in *Petunia* depends on two major genetic loci for floral scent production. *Curr Biol* 21:730-739.
- Kim JY, Swanson RT, Alvarez MI, Johnson TS, Cho KH, Clark DG and Colquhoun TA (2019) Down regulation of p-coumarate 3-hydroxylase in *Petunia* uniquely alters the profile of emitted floral volatiles. *Sci Rep* 9:8852.
- Knapp S (2010) On 'various contrivances': pollination phylogeny and flower form in the Solanaceae. *Philos Transact R Soc* 365:449-460.
- Knudsen JT and Gershenzon J (2006) The chemical diversity of floral scent. In: Dudareva N, Pichersky E (eds) *Biology of floral scent*. CRC Press, Boca Raton, pp 27-44.
- Knudsen JT, Eriksson R, Gershenzon J and Ståhl B (2006) Diversity and distribution of floral scent. *Bot Rev* 72:1-120.
- Koeduka T, Fridman E, Gang DR, Vassão DG, Jackson BL, Kish CM, Orlova I, Spassova SM, Lewis NG, Noel JP *et al.* (2006) Eugenol and isoeugenol, characteristic aromatic constituents of spices, are biosynthesized via reduction of a coniferyl alcohol ester. *Proc Natl Acad Sci U S A* 103:10128-10133.
- Larsson A (2014) AliView: A fast and lightweight alignment viewer and editor for large data sets. *Bioinformatics* 30:3276-3278.
- Laskowski RA, MacArthur MW, Moss DS and Thornton JM (1993) PROCHECK - a program to check the stereochemical quality of protein structures. *J Appl Cryst* 26:283-291.
- Löytynoja A and Goldman N (2005) An algorithm for progressive multiple alignment of sequences with insertions. *Proc Natl Acad Sci U S A* 102:10557-10562.
- Lunau K (2004) Adaptive radiation and coevolution - pollination biology case studies. *Org Divers Evol* 4:207-224.
- Luo J, Nishiyama Y, Fuell C, Taguchi G, Elliott K, Hill L, Tanaka Y, Kitayama M, Yamazaki M, Bailey P *et al.* (2007) Convergent evolution in the BAHD family of acyl transferases: identification and characterization of anthocyanin acyl transferases from *Arabidopsis thaliana*. *Plant J* 50:678-695.
- Lüthy R, Bowie JU and Eisenberg D (1992) Assessment of protein models with three-dimensional profiles. *Nature* 356:83-85.
- Ma X, Koepke J, Panjkar S, Fritzsche G and Stockigt J (2005) Crystal structure of vinorine synthase, the first representative of the BAHD superfamily. *J Biol Chem* 280:13576-13583.
- Maere S, De Bodt S, Raes J, Casneuf T, Van Montagu M, Kuiper M and van de Peer Y (2005) Modeling gene and genome duplications in eukaryotes. *Proc. Nat Acad Sci U S A* 102:5454-5459.
- Morris AL, MacArthur MW, Hutchinson EG and Thornton JM (1992) Stereochemical quality of protein structure coordinates. *Proteins: Struct Funct Bioinf* 12:345-364.
- NCBI Resource Coordinators (2016) Database resources of the National Center for Biotechnology Information. *Nucleic Acids Res* 44:D7-D19.
- Olmstead RG, Bohs L, Rigid HA, Santiago-Valentin E, Garcia VF and Collier SM (2008) Molecular phylogeny of the Solanaceae. *Taxon* 57:1159-1181.
- Orlova I, Marshall-Colon A, Schnepf J, Wood B, Varbanova M, Fridman E, Blakeslee JJ, Peer WA, Murphy AS, Rhodes D *et al.* (2006) Reduction of benzenoid synthesis in *Petunia* flowers reveals multiple pathways to benzoic acid and enhancement in auxin transport. *Plant Cell* 18:3458-3475.
- Rachersberger M, Cordeiro G, Schäffler I and Dotterl S (2019) Honeybee pollinators use visual and floral scent cues to find apple (*Malus domestica*) flowers. *J Agric Food Chem* 67:13221-13227.
- Raguso RA (2001) Floral scent, olfaction, and scent-driven foraging behavior. In: Chittka L, Thomson DJ (eds) *Cognitive ecology of pollination. Animal behavior and floral evolution*. Cambridge University Press, Cambridge, pp 91-92.
- Ramakrishnan C and Ramachandran GN (1965) Stereochemical criteria for polypeptide and protein chain conformations. *Biophys J* 5:909-933.
- Rodrigues DM, Caballero-Villalobos LM, Turchetto C, Jacques RA, Kuhlemeier C and Freitas LB (2018) Do we truly understand pollination syndromes in *Petunia* as much as we suppose? *AoB Plants* 10:ply057
- Ronquist F, Teslenko M, van der Mark P, Ayres D, Darling A, Höhna S, Larget B, Liu L, Suchard MA and Huelsenbeck JP (2011) MrBayes 3.2: efficient Bayesian phylogenetic inference and model choice across a large model space. *Syst Biol* 61:539-542.
- Sali A and Blundell TL (1993) Comparative protein modelling by satisfaction of spatial restraints. *J Mol Biol* 234:779-815.
- Sánchez R and Sali A (1997) Advances in comparative protein-structure modelling. *Curr Opin Struct Biol* 7:206-214.

- Särkinen T, Bohs L, Olmstead RG and Knapp S (2013) A phylogenetic framework for evolutionary study of the nightshades (Solanaceae) a dated 1000-tip tree. *BMC Evol Biol* 13:214.
- Schiestl FP and Johnson SD (2013) Pollinator-mediated evolution of floral signals. *Trends Ecol Evol* 28:307-315.
- Segatto ALA, Ramos-Fregonezi AMC, Bonatto SL and Freitas LB (2014) Molecular insights into the purple-flowered ancestor of garden petunias. *Am J Bot* 101:119-127.
- Segatto ALA, Thompson CE and Freitas LB (2016a) Contribution of *WUSCHEL*-related homeobox (WOX) genes to identify the phylogenetic relationships among *Petunia* species. *Genet Mol Biol* 39:658-664.
- Segatto ALA, Thompson CE and Freitas LB (2016b) Molecular evolution analysis of *WUSCHEL*-related homeobox transcription factor family reveals functional divergence among clades in the homeobox region. *Dev Genes Evol* 226:259-268.
- Stehmann JR, Lorenz-Lemke AP, Freitas LB and Semir J (2009) The genus *Petunia*. In: Gerats T, Strommer J (eds) *Petunia: evolutionary, developmental and physiological genetics*. Springer, New York, pp 1-28.
- The UniProt Consortium (2017) UniProt: The universal protein knowledgebase. *Nucleic Acids Res* 45:D158-D169.
- Tuominen LK, Johnson VE and Tsai CJ (2011) Differential phylogenetic expansions in BAHD acyltransferases across five angiosperm taxa and evidence of divergent expression among *Populus* paralogues. *BMC Genomics* 12:236.
- Vandenbussche M, Chambrier P, Rodrigues-Bento S and Morel P (2016) *Petunia*, your next supermodel? *Front Plant Sci* 7:72.
- Venail J, Dell'Olivo A and Kuhlemeier C (2010) Speciation genes in the genus *Petunia*. *Philos Trans R Soc Lond B Biol Sci* 365:461-468.
- Wang C, Li J, Ma M, Lin Z, Hu W, Lin W and Zhang P (2021) Structural and biochemical insights into two BAHD acyltransferases (AtSHT and AtSDT) involved in phenolamide biosynthesis. *Front Plant Sci* 11:610118.
- Webb B and Sali A (2014) Comparative protein structure modeling using Modeller. *Curr Protoc Bioinform* 47:5.6.1-5.6.32.
- Wiltgen M (2018) Algorithms for structure comparison and analysis: Homology modelling of proteins. In: Ranganathan S, Gribskov M, Nakai K and Schönbach C (eds) *Encyclopedia of Bioinformatics and Computational Biology*, Elsevier, Cambridge, vol. 1, pp 38-61.
- Yockteng R, Almeida AMR, Morioka K, Alvarez-Buylla ER and Specht CD (2013) Molecular evolution and patterns of duplication in the SEP/AGL6-like lineage of the Zingiberales: A proposed mechanism for floral diversification. *Mol Biol Evol* 30:2401-2422.
- Yu X-H, Gou J-Y and Liu C-J (2009) BAHD superfamily of acyl-CoA dependent acyltransferases in *Populus* and *Arabidopsis*: bioinformatics and gene expression. *Plant Mol Biol* 70:421-442.
- Zhang T, Huo T, Ding A, Hao R, Wang J, Cheng T, Bao F and Zhang Q (2019) Genome-wide identification, characterization, expression and enzyme activity analysis of coniferyl alcohol acetyltransferase genes involved in eugenol biosynthesis in *Prunus mume*. *PLoS One* 14:e0223974.

Internet Resources

- AliView (2021) <http://www.ormbunkar.se/aliview/> (accessed 4 March 2022).
- ExPASy Tools (2020) https://web.expasy.org/compute_pi/ (accessed 4 March 2022).
- HMMER (2020) <https://www.ebi.ac.uk/Tools/hmmer/> (accessed 4 March 2022).
- MAFFT (2021) <http://mafft.cbrc.jp/alignment/software/> (accessed 4 March 2022).
- MODELLER (2022) <https://salilab.org/modeller/> (accessed 4 March 2022).
- MrBayes (2019) <http://mrbayes.sourceforge.net/> (accessed 4 March 2022).
- NCBI (2022) <https://www.ncbi.nlm.nih.gov/> (accessed 4 March 2022).
- PDB (2022) <http://www.rcsb.org/pdb/home/home.do> (accessed 4 March 2022).
- Pfam (2022) <http://pfam.xfam.org/> (accessed 4 March 2022).
- PRANK (2022) <https://www.ebi.ac.uk/goldman-srv/webprank/> (accessed 4 March 2022).
- PROCHECK (2010) <https://www.ebi.ac.uk/thornton-srv/software/procheck/> (accessed 4 March 2022).
- PyMol (2022) <https://pymol.org/> (accessed 4 March 2022).
- UniProtKB (2017) <https://www.uniprot.org/help/uniprotkb> (accessed 4 March 2022).
- Verify 3D (2021) <https://www.doe-mbi.ucla.edu/verify3d/> (accessed 4 March 2022).

Supplementary material

The following online material is available for this article: Table S1 – Protein sequences included in evolutionary analysis of volatile organic compounds in Solanaceae.

Associate Editor: Rogerio Margis

License information: This is an open-access article distributed under the terms of the Creative Commons Attribution License (type CC-BY), which permits unrestricted use, distribution and reproduction in any medium, provided the original article is properly cited.